STRUCTURAL PROPERTIES OF HYDROGENATED AMORPHOUS SILICON (a-Si:H) THIN FILM GROWN VIA RADIO FREQUENCY PLASMA ENHANCED CHEMICAL VAPOR DEPOSITION (RF PECVD)

HASBULLAH BIN ANTHONY HASBI

A thesis submitted in fulfilment of the
requirements for the award of the degree of
Master of Science (Physics)

Faculty of Science
Universiti Teknologi Malaysia

JUNE 2005

To

My parents Anthony Hasbi and Paimah Junaidi

for setting me on the path toward intellectual pursuits

My sisters Hasmah, Hasmiah and Hazalimah

for their continuing support along the way

My friends

for making the journey so enjoyable.

ACKNOWLEDGEMENT

I would like to acknowledge the large number of people, too numerous to mention individually, who have stimulated my interest in this research over the past two years. I would particularly like to thank my project supervisor, Associate Prof. Dr. Zulkafli Othaman and co-supervisor Prof. Dr. Samsudi Sakrani for their suggestions and indirect encouragement in this venture.

Furthermore, this thesis would not have been possible without the very pleasant and creative working atmosphere that prevails at the Vacuum and Research Laboratory, Department of Physics, UTM Skudai. I would like these lines to be an expression of my gratitude to my colleagues and my pals especially Lau Yee Chen and Suriani. Not forgetting lab attendance Mr. Nazri, Kak Wani and Mr. Jaafar. Their help has turn out to be inestimably important.

My thanks to Prof. John Wilson, Academic Head of Physics, Schools of Engineering and Physical Sciences, Heriot-Watt University, Edinburgh, UK for his support and guidance. I really appreciate the helpful discussions and assistance along my attachment program at Heriot-Watt. Not forgetting all the members of Diamond Group who've helped me with the use of some of the equipments. Their constant help and support made all the months I've spent there one of the best experiences in my life.

The working and writing of this project has been at the expense of many hours and miles away from my loving parent. It is dedicated to you, Mom and Dad.

ABSTRACT

An investigation of the structural properties of hydrogenated amorphous silicon (a-Si:H) thin films prepared by plasma enhanced chemical vapour deposition of silane (SiH_4) was done using a combination of atomic force microscopy (AFM), photoluminescence, infrared and UV spectroscopy. Films were prepared with rf power ranging from 100-250 W. For every rf power employed, substrate temperature were varied from room temperature to 300˚C. The deposition rate was found to be slightly increasing with an increase of rf power while decreasing as the substrate temperature increases. The AFM images can be classified into three groups: most smooth (rms: 1.2nm), intermediate rms (2.4-3.6 nm) and highest roughness (rms: 4.9 nm). The transition to rougher films at higher substrate temperature is attributed to a change in the deposition process. The IR vibrational spectra obtained from FTIR spectroscopy display modes which can be characterized as predominantly hydrogen motions. On the basis of these identifications, it is found that samples produced on high-temperature have SiH, SiH_2 and $(SiH_2)_n$ groups with very little SiH_3. In contrast, the ir spectra of samples produced on room-temperature are dominated by vibrational modes of SiH_3 and $(SiH_2)_n$. At low rf power, the spectrum is dominated by a strong absorption bands at 2000 cm^{-1} associated with SiH stretching bond and also 630 cm^{-1} associated with SiH bending. At high rf power, an additional absorption band at around 2090 cm^{-1} which corresponds to $(SiH_2)_n$ stretching mode and SiH_2 stretching mode becomes more pronounced. The optical energy gap obtained from UV spectroscopy decreases with increasing of rf power and substrate temperature. This decrement is due to the drop of hydrogen content. At low substrate temperature, photoluminescence spectrum of a-Si consists of a relatively broad band with its main peak around 1.4 eV. The spectrum shifts to lower energies (around 1.37 eV) and its intensity decreases with increasing temperature. It is suggested that this is due to an activated non-radiative recombination (relaxation) process where exciton are captured by deep traps and this become more probable as temperature increases.

ABSTRAK

Satu kajian tentang struktur bahan saput tipis amorfus silikon terhidrogenasi (a-Si:H) yang disediakan melalui kaedah pemendapan wap kimia diperkuat plasma dengan gas silane (SiH_4) telah dijalankan melalui kombinasi kaedah Mikroskopi Daya Atom (MDA), fotoluminesen serta spektroskopi inframerah (IM) dan ultralembayung. Saput telah disediakan dengan kuasa frekusi radio (fr) dari 100-250 W. Bagi setiap kuasa fr yang dikenakan, suhu substrate diubah dari suhu bilik ke 300˚C. Kadar pemendapan didapati meningkat dengan setiap penambahan kuasa fr manakala ianya menurun apabila suhu substrat meningkat. Imej MDA yang dicerap boleh diklasifikasikan kepada tiga kumpulan: paling halus (rms 1.2 nm), rms pertengahan (2.4-3.6 nm) dan paling kasar (rms 4.9 nm). Transisi ke saput yang lebih kasar adalah disebabkan prubahan yang berlaku dalam proses pemendapan. Spektrum yang diperolehi daripada spektroskopi inframerah memaparkan mod yang boleh dicirikan sebagai gerakan hidrogen. Melalui identifikasi ini, didapati sampel yang disediakan dalam suhu tinggi mempunyai kumpulan SiH, SiH_2 dan $(SiH_2)_n$ dengan sedikit SiH_3. Sebaliknya, dalam suhu bilik didapati spektrum didominasi oleh mod getaran SiH_3 dan $(SiH_2)_n$. Pada kuasa fr rendah, spektrum didominasi oleh jalur serapan yang kuat pada 2000 cm^{-1} dikaitkan dengan ikatan regangan SiH dan 630 cm^{-1} dikaitkan dengan bengkokan SiH. Manakala pada kuasa fr yang tinggi, satu jalur serapan sekitar 2090 cm^{-1} dikaitkan dengan mod regangan $(SiH_2)_n$ dan SiH_2 didapati semakin ketara. Jurang tenaga optik yang diperolehi melalui spektroskopi ultralembayung menurun dengan peningkatan kuasa fr dan suhu substrat. Ini disebabkan oleh menurunnya jumlah hidrogen yang terkandung dalam sampel. Pada suhu substrat yang rendah, spektrum fotoluminesen a-Si memaparkan jalur lebar dengan puncak utama sekitar 1.4 eV. Puncak spectrum menurun ke tenaga yang lebih rendah (sekitar 1.37 eV) manakala keamatannya berkurang dengan peningkatan suhu substrat. Ini adalah disebabkan oleh teraktifnya proses penggabungan semula tanpa pemancaran (santaian) di mana *exciton* diperangkap oleh perangkap dalam pada jurang tenaga dan proses ini menjadi lebih mudah terjadi dengan peningkatan suhu substrat.

TABLE OF CONTENTS

CHAPTER	TITLE	PAGE
	DECLARATION	ii
	ACKNOWLEDGEMENT	iv
	ABSTRACT	v
	ABSTRAK	vi
	TABLE OF CONTENTS	vii
	LIST OF TABLES	x
	LIST OF FIGURES	xi
	LIST OF SYMBOLS	xv
1	**INTRODUCTION**	
	1.1 Amorphous Semiconductor	1
	1.2 Potential Applications	2
	1.3 Research Objectives	5
	1.4 Research Scope	5
	1.5 Layout of Thesis	5
2	**LITERATURE REVIEW**	
	2.1 Hydrogenated Amorphous Silicon (a-Si:H)	7
	2.1 Hydrogenation of a-Si	8
	2.2 Conventional Thin Film Deposition Techniques	13

2.2.1 Chemical Vapor Deposition 13
2.2.2 DC Glow Discharge 14
2.2.3 RF Glow Discharge 18
2.3 Plasma Enhanced Chemical Vapor Deposition (PECVD) 19
2.4 Plasma Fundamentals 19
2.4.1 Non-equilibrium Glow Discharges 19
2.4.2 Potentials in rf Glow Discharges 21
2.5 Qualitative Model for PECVD Reactions 22

3 METHODOLOGY

3.1 Deposition of Amorphous Silicon Films 27
3.1.1 Introduction 27
3.1.2 Plasma Enhanced Chemical Vapor Deposition 27
3.1.3 PECVD Setup 28
3.1.4 PECVD System Deposition Process 33
3.1.5 Preparation of a-Si:H Samples 34
3.1.5.1 Substrate Preparation 34
3.1.5.2 Deposition Parameters 34
3.2 Analytical Tools 36
3.2.1 Spectroscopy 36
3.2.2 Absorption 37
3.2.2.1 Optical Absorption 37
3.2.2.2 UV-3101-PC Spectrophotometer 42
3.2.3 Infrared (IR) Absorption Spectroscopy 45
3.2.3.1 Introduction 45
3.2.3.2 Mechanism of IR Absorption 45
3.2.3.3 FTIR – Fourier Transform Infrared Spectroscopy 46
3.2.4 Photoluminescence 49
3.2.4.1 Basic Theory of Photoluminescence 49
3.2.4.2 Luminescence Spectrometer LS 55 51
3.2.5 Atomic Force Microscopy (AFM) 54

3.2.5.1 Contact Mode 56
3.2.5.2 Non-contact Mode 57
3.2.5.3 Tapping Mode 57
3.2.5.4 Image Display 57
3.2.5.5 Surface Roughness 58
3.3 Film Thickness Measurements 58

4 RESULTS AND DISCUSSIONS

4.1 Surface Morphology and Deposition Rate 61
4.2 X-Ray Diffraction (XRD) Analysis 70
4.3 Infrared (IR) Transmission Spectrum 72
4.3.1 Dependence on rf Power 74
4.3.2 Dependence on Substrate Temperature 79
4.4 Optical Energy Gap 84
4.5 Photoluminescence 89
4.5.1 Dependence on Substrate Temperature 89

5 CONCLUSION

5.1 Summary 96
5.2 Recommendation 98

REFERENCES 99

PRESENTATIONS 105

LIST OF TABLE

TABLE NO.	TITLE	PAGE
3.1	The preparation conditions for a-Si:H thin films under different RF power and substrate temperature. Note that other parameters are kept constant.	35
4.1	The observed mode frequency and their assignments.	72

LIST OF FIGURES

FIGURE NO.	TITLE	PAGE
1.1	Schematic representation of a typical thin film a-Si:H solar cell on glass. The incoming photons with an energy larger than the band gap are absorbed in the intrinsic a-Si:H film creating holes-electron pairs.	3
1.2	Schematic of a general active matrix array.	4
2.1	A model of hydrogenated amorphous silicon. The small ball represent hydrogen atoms while the large ball represents silicon atoms.	9
2.2	Model for the adsorption, diffusion and recombination of SiH_3 on the growing surface.	12
2.3	A common implementation of CVD (AX, X, BX – gases, AB – solid material).	14
2.4	Current-voltage characteristics in a DC glow discharge.	15
2.5	Luminous zones and dark spaces in a DC glow discharges.	16
2.6	The potential distribution in a DC glow discharge. (V_p – plasma potential, V_c – cathode potential).	17
2.7	Schematic of fundamental transport and reaction processes underlying CVD.	23
2.8	Equivalent circuit representation of the sequence of steps in thermally driven CVD. The R_i (with i = 1-7) represent the seven steps describe in the text.	24
2.9	Equivalent circuit representation showing the thermal CVD path, and the parallel plasma-enhanced path	

	represented by the R_i^*s.	25
2.10	Activation energy diagram for a thermally driven (solid line) and plasma enhanced (dashed line) reaction. The activation energy for the plasma enhanced reaction, ΔE^*, is typically less than that for the thermally driven reaction, ΔE.	26
3.1	NPN_2 gas.	29
3.2	PN_2 gas rack.	29
3.3	Silane (SiH_4) gas cabinet.	30
3.4	Scrubber.	30
3.5	Schematic of the rf PECVD reactor system.	31
3.6	The rf PECVD reactor system.	32
3.7	A schematic of the optical absorption curves of amorphous materials.	39
3.8	Electron transition for semiconductors having a direct gap and indirect gap	40
3.9	Shimadzu UV-3101-PC Spectrophotometer.	44
3.10	Examples of infrared active and inactive absorption bands in CO_2.	46
3.11	Fourier transform infrared spectrometer (Perkin Elmer Spectrum GX).	48
3.12	A schematic of the PL process.	50
3.13	Photoluminescence spectrometer LS 55.	52
3.14	Luminescence spectrometer schematic diagram.	54
3.15	Beam deflection system, using a laser and photodetector to measure the beam position.	55
3.16	Force between tip and sample surface	56
3.17	Colour mapping scheme for height	58
3.18	Dektak3 surface profiler.	59
4.1	Representation of surface morphology of a-Si:H films.	63
4.2	The 10 μm × 10 μm AFM images with surface height given by the grey scales extending from 0 (black) to 400 nm (white): (a) sample A deposited at 27°C; (b) sample B deposited at 100°C; (c) sample C	

	deposited at 200°C; (d) sample D deposited at 300°C.	64
4.3	Deposition rate of a-Si:H films deposited at different temperature as a function of rf power.	67
4.4	Deposition rate of a-Si:H films deposited at different rf power as a function of substrate temperature.	68
4.5	Model of surface reaction where Si-Si is formed releasing H_2.	69
4.6	X-ray diffraction pattern of a-Si:H thin film deposited at room temperature and rf power of 100 W.	70
4.7	X-ray diffraction pattern of a-Si:H thin film deposited at 200˚C and rf power of 50 W.	71
4.8	Local Si-H vibrations for SiH, SiH_2 and SiH_3 groups.	72
4.9	IR transmission of a-Si:H thin films deposited at different rf power. Emphasize on the 2000 cm^{-1} regime.	75
4.10	IR transmission of a-Si:H thin films deposited at different rf power. Emphasize on the 600 cm^{-1} regime.	76
4.11	IR transmission of a-Si:H thin films deposited at different rf power. Emphasize on the 800 cm^{-1} regime.	77
4.12	IR transmission of a-Si:H thin film prepared under different rf power by Lucovsky *et al.* (1979)	78
4.13	IR transmission of a-Si:H thin films deposited at different substrate temperatures. Emphasize on the 2000 cm^{-1} regime. RF power is at 100 W.	81
4.14	IR transmission of a-Si:H thin films deposited at different substrate temperatures. Emphasize on the 800 cm^{-1} regime. RF power is at 100 W.	82
4.15	IR transmission of a-Si:H thin films deposited at different substrate temperatures. Emphasize on the 600 cm^{-1} regime. RF power is at 100 W.	83
4.16	The $(\alpha h\nu)^{1/2}$ vs $h\nu$ graphs for a-Si:H deposited at different rf power.	84
4.17	The $(\alpha h\nu)^{1/2}$ vs $h\nu$ graphs for a-Si:H deposited at different substrate temperature.	85
4.18	Energy gap of a-Si:H films prepared under different	

	substrates temperatures as a function of rf power.	86
4.19	Luminescence spectrum of amorphous silicon at various substrate temperatures with rf power kept constant at 50W.	90
4.20	Luminescence spectrum of amorphous silicon at various substrate temperatures with rf power kept constant at 100W.	91
4.21	Luminescence spectrum of amorphous silicon at various substrate temperatures with rf power kept constant at 150W.	91
4.22	Luminescence spectrum of amorphous silicon at various substrate temperatures with rf power kept constant at 200W.	92
4.23	Luminescence spectrum of amorphous silicon at various substrate temperatures with rf power kept constant at 250W.	92
4.24	Flow diagram representing the interrelation of the excitation and recombination processes appropriate to amorphous silicon.	94
4.25	Schematic plot of the relaxation and recombination probabilities versus energy from midgap.	95

LIST OF SYMBOL

V_B	-	Breakdown voltage
V_G	-	Glow discharge voltage
V_p	-	Plasma potential
V_c	-	Cathode potential
V_f	-	Floating potential
A	-	Gas species
A^*	-	Reactive species
e^-	-	Electrons
e	-	Unit electron charge (1.60×10^{-19} C)
k_1	-	Reaction rate coefficient
T_e	-	Electron temperature
T_s	-	Substrate temperature
m_i	-	Ion mass
m_e	-	Electron mass
k	-	Boltzmann constant (1.38×10^{-23} J/K)
ΔE^*	-	Activation energy for plasma enhanced reaction
ΔE	-	Thermally driven activation energy
E_g	-	Optical gap
E_o	-	Urbach energy
α	-	Optical absorption
h	-	Planck constant (6.625×10^{-34} J-s)
ν	-	Frequency
B	-	Edge width parameter
A	-	Absorbance
T	-	Transmittance
I_o	-	Incident light intensity

I	-	Intensity of light transmitted through sample
d	-	Film thickness
t	-	Deposition time
c	-	Speed of light (2.998×10^8 m/s)
λ	-	Wavelength of light
D_s	-	Surface diffusion
τ_s	-	Staying time
dr	-	Deposition rate
C_H	-	Bonded H content
X_C	-	Volume fraction of microcrystalline

CHAPTER 1

INTRODUCTION

1.1 Amorphous Semiconductor

Amorphous semiconductors are noncrystalline and have significantly different characteristics than those of crystalline (Street, 1991). They lack long-range periodic ordering of their constituent atoms. That is not to say that amorphous semiconductors are completely disordered on the atomic scale.

Local chemistry provides almost rigorous bond-length and a lesser extent, bond-angle constraint on the nearest-neighbor environment. Unlike amorphous metals, amorphous semiconductor do not consist of close-packed atoms, but rather they contain covalently bonded atoms arranged in an open network with correlations in ordering up to the third or fourth nearest neighbors. The short-range order is directly responsible for observable semiconductor properties such as optical absorption edges and activated electrical conductivities.

Amorphous semiconductors are usually fabricated in the form of thin films by an atomic deposition procedure such as evaporation, sputtering, chemical vapor deposition, and plasma decomposition on gases or electroplating. Sometimes ion bombardment of crystals is used to have an amorphous layer in the collision trail of the ions.

1.2 Potential Applications

The commercial potential of amorphous semiconductors has encouraged many to study their properties and preparation. In particular, hydrogenated amorphous silicon (a-Si:H) is very versatile, low cost material that has made it desirable for the use in many device applications. Other special attribute of a-Si:H is the ability to deposit the material inexpensively over large areas.

In recent years, the development of thin film a-Si:H photovoltaic solar cells has been extensively pursued because such devices offer the potential of low-cost electricity, making them attractive as a source of utility and residential electric power. Single-junction a-Si:H p-i-n solar cells with solar energy conversion efficiency of 10% have been achieved by several laboratories (Shen *et al.* 1991). The basic structure of a single-junction a-Si:H p-i-n cell consists of a very thin (less than 10 nm thick, p-type layer), low-defect, 200 to 600 nm thick intrinsic layer, and a thin (about 30 nm thick) n-type layer. The construction of a basic single junction thin film a-Si:H solar cell is illustrated in Figure 1.1. To improve efficiency and stability of a-Si:H solar cells, multiple-junction solar cell structures using a-Si:H alloys are being extensively studied (Yang *et al.* 1997).

The need for large-area charged particle and X-ray detectors for applications like medical imaging and calorimetry in high-energy physics experiments have stimulated significant investigations into using a-Si:H (50 to 70 µm thick) for such applications (Xi *et al.* 1991). Other photodiode applications for a-Si:H alloys include ultraviolet light detectors (Krause *et al.* 2001), edge detector for application to neural network image sensors (Sah *et al.* 1990), and position sensors for telephone terminals (Brida *et al.* 2002).

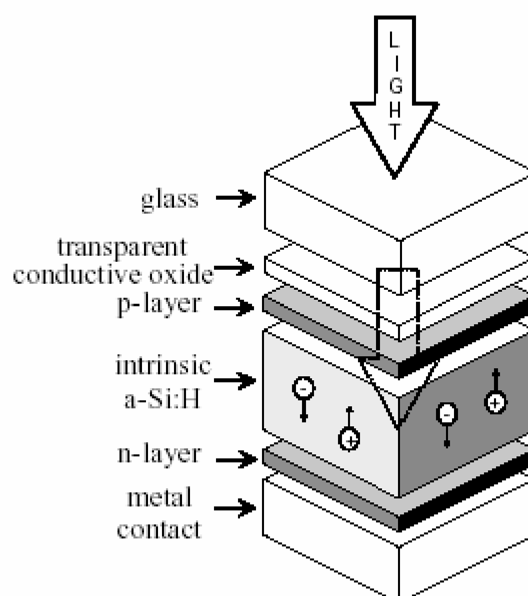

Figure 1.1: Schematic representation of a typical thin film a-Si:H solar cell on glass. The incoming photons with an energy larger than the band gap are absorbed in the intrinsic a-Si:H film creating holes-electron pairs.

The most attractive applications of a-Si:H technology are active matrix displays and active matrix flat-panel imagers (AMFPIs) (Zhao *et al.* 1995) which are collectively termed as active matrix arrays (Figure 1.2). Active matrix arrays contain many individual elements commonly known as pixels, which are generally addressed or read out by a grid structure of interconnecting lines termed gate and data lines. In these applications, an a-Si:H thin film transistor (TFT) is used as a switching element or pass transistor. The active matrix arrays require external chips to multiplex and drive the large number of gate and data lines. Considering the growing applications of the active matrix displays and imaging arrays, a low cost on-chip solution is needed for the multiplexer and driver circuitry. Designing of the multiplexer and driver circuits in a-Si:H technology requires the specific details of the displays and imaging arrays.

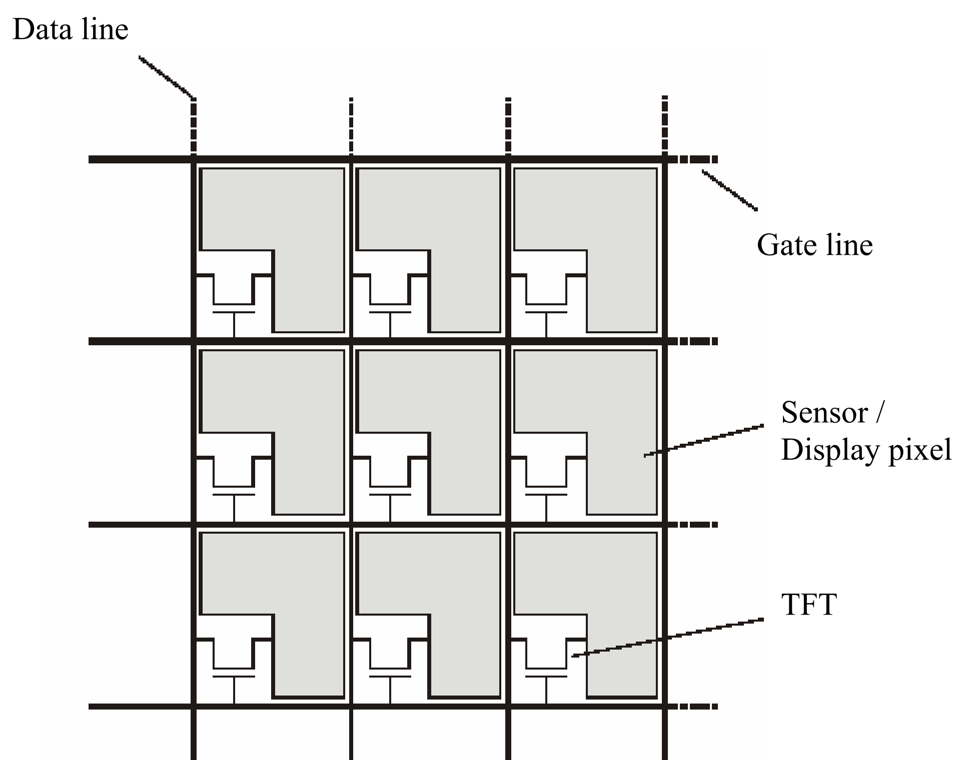

Figure 1.2: Schematic of a general active matrix array

The unique properties of a-Si:H depend primarily on the complex structure involving different bonding configurations and on the incorporation of hydrogen in the films. Hydrogen, being a terminator in the carbon network, plays a crucial role in determining the properties of the films. The structure of, and the incorporation of hydrogen in a-Si:H films are critically determined by the energy of the ionic species and the consumption of the gas mixture in the deposition process. The ion energy can be changed by varying the deposition parameters. Therefore, it is feasible to obtain a-Si:H films with a wide range of properties by adjusting the deposition parameters in the growth process.

1.3 Research Objectives

The main purpose of this work is to deposit hydrogenated amorphous silicon (a-Si:H) thin films using silane (SiH_4) gas as film precursor via plasma enhanced chemical vapor deposition (PECVD) technique. Secondly, to study the structural characteristics of hydrogenated amorphous silicon (a-Si:H) thin films and to acquire better understanding of this material by characterisation techniques using surface profiler, atomic force microscopy (AFM), UV spectrophotometer, Fourier Transform Infrared (FTIR) spectroscopy, X-ray diffraction (XRD) and photoluminescence spectrometer. In order to do so, the effect of deposition conditions on the grown film properties is investigated.

1.4 Research Scope

Hydrogenated amorphous silicon thin films are deposited using rf-PECVD with silane (SiH_4) gas as film precursor under different substrate temperature and rf power while other parameters kept constant. The films are then structurally characterized using pre-determined characterization techniques which consist of;

- Surface profiler
- Atomic force microscopy (AFM)
- UV spectrophotometer
- Fourier Transform Infrared (FTIR) spectroscopy
- X-ray diffraction (XRD)
- Photoluminescence spectrometer

1.5 Layout of Thesis

This thesis is organized as follows. In Chapter 1, some of the previous related works on hydrogenated amorphous silicon (a-Si:H) and its application are reviewed. This chapter also ruled out the objectives of conducting the research.

Following the introduction chapter, the literature survey is presented in Chapter 2. This will cover the growth of a-Si:H thin film process, the fundamental of deposition technique which is the plasma enhanced chemical vapor deposition (PECVD) and the reaction process in this technique.

Details of experimental methods, including fabrication of the films, PECVD setups are given in the initial part of Chapter 3. This is followed by the characterization techniques used, namely UV spectroscopy, FTIR spectroscopy and photoluminescence.

Chapter 4 presents the results obtained in this work. Among the characterization results that would be presented are the surface morphology and deposition rate, IR transmission spectrum, optical energy gap and photoluminescence. Effect of varying deposition parameters on the film characteristics will also be discussed in this chapter.

Finally, the conclusions of the project are made in Chapter 5. These include the summarization of the whole project and some recommendations for future work are also suggested.

the exciton makes its capture by deep traps more probable; hence, radiative channel becomes insignificant. In addition, as temperature increases, relaxation (non-radiative recombination) is more probable than radiative recombination, giving the centre mass of luminescence spectrum moved to lower energy.

5.2 Recommendation

In this study, the hydrogenated amorphous silicon thin films were prepared under different rf powers and substrate temperatures. For future works, it is suggested that imposing other parameters such as chamber pressure and precursor gas flow rate would also be considered as these parameters are also believed to give a significant change in the structure of the amorphous film grown.

In addition, instead of only focusing on the intrinsic amorphous silicon thin film, study can also be done on doped amorphous silicon thin film since doped materials are pretty much important mainly in developing thin film devices such as solar cells. This can be made possible by mixing doping gas precursor namely diborane (B_2H_6) and phosphane (P_2H_4) with silane (SiH_4) during deposition process.

There are many ways to study the structural characteristic of amorphous thin film. Other than the techniques mentioned in this thesis, the amorphous silicon thin films can also be characterised by using Scanning Electron Microscopy (SEM) or Tunneling Electron Microscopy (TEM) since these characterisation equipments are able to give detail on the surface morphology of the films. This would in turn compliment the AFM results that have been obtained.

REFERENCES

Adams, A. C. (1983). Plasma Deposited Hydrogenated Amorphous Silicon Nitride Thin Films. *Solid State Technology.* 26(4): 135-140.

Bellamy, L. J. (1975). *The Infra-Red Spectra of Complex Molecules*. London: Chapman and Hall.

Brida, D., Fortunato, E., Aguas, H., Silva, V., Marques, A., Pereira, L., Ferreira, I. and Martins, R. (2002). New Insights on Large Area Flexible Position Sensitive Detectors. *J. Non-Cryst. Solids*, 299: 1272-1276.

Brodsky, M. H., Cordona, M., Cuomo, J. J. (1977). Infrared and Raman Spectra of The Silicon-hydrogen bonds in a-Si Prepared by Glow Discharge and Sputtering. *Phys. Rev. B*. 16(8): 3556-3571.

Brodsky, M. H. and Title, R. S. (1969). On The Deposition of Amorphous Silicon Films from Glow Discharge Plasmas of Silane. *Phys. Rev. Lett.* 23: 581-585.

Bunshah, R. F. (1993). *Handbook of Deposition Technologies for Films and Coatings.* Park Bridge, N. J.: Noyes Publications.

Chapman, B. (1980). *Glow Discharge Processes.* New York: John Wiley.

Chittig, R. C., Alexander, J. H., Sterling, H. F. (1969). The Preparation and Properties of Amorphous Silicon. *J. of Electrochem. Soc.* 116: 77-81.

Drevillon, G., Huc, J., Lort, A., Perrin, J., de Rosny, G., and Schimtt, J. P. M. (1980). Silane Dissociation Mechanisms and Thin Film Formation in a Low Pressure Multipole DC Discharge. *Appl. Phys. Lett.* 37:646-648.

Dutta, R., Banarjee, P. K. and Mitra, S. S. (1982). Optical and Electrical Properties of Hydrogenated Amorphous Silicon Carbide. *Phys. Stat. Sol. B*. 113(1): 277-284.

Engemann, D. and Fischer, R. (1977). Photoluminescence in Amorphous Silicon. *Phy. Stat. Sol. (B),* 79: 195-202.

Fischer, R., Heim, U., Stern, F., and Weiser, K. (1971). Photoluminescence of Amorphous $2As_2Te_3 \cdot As_2Se_3$ Films. *Phys. Rev. Lett*., 26(19): 1182-1185.

Goh, F. H. C. (1992). *Wide Bandgap Amorphous Silicon-based Alloys Using PECVD*. University of Arkansas: Ph.D. Thesis.

Gorowitz, B., Gorczyca, T. B. and Saia, R. J. (1985). Amorphous Silicon Nitride Deposition Rates in RF Glow Discharges. *Solid State Technology.* 28(6): 197-200.

Hadjadj, A., Beorchia, A.,Rocca I Cabarrocas, P., Boufendi, L., Heut, S. and Budendorff, J. L. (2001). Effects of the Substrate Temperature on the Growth and Properties of hydrogenated nanostructured silicon thin films. *J. Phys. D: Appl. Phys.,* 34: 690-699.

Hata, N., Yamasaka, S., Oheda, H., Matsuda, A., Okushi, H. and Tanaka, K. (1981). A Photoluminescence Study of Amorphous-Microcrystalline Mixed-Phase Si:H Films. *Jpn. J. Appl. Phys.*, 20(11): L793-796.

Hollahan, J. R. and Rosler, R. S. (1978). In: Vossen, J. L. and Kern, W. ed. *Thin Film Processes*. New York: Academic Press. Ch. IV-1.

Howatson, A. M. (1976). *An Introduction to Gas Discharges.* Oxford: Pergamon Press.

Inoue, G. and Suzuki, M. (1985). Reactions of SiH_2 ($X'A_1$) with H_2, CH_4, C_2H_4, SiH_4 and Si_2H_6 at 298 K. *Chemical Phys. Lett.* 122: 361-364.

Janai, M., Weil, R. and Levin, H. K. (1981). Optical Properties of Fluorinated Glow-Discharge Amorphous Silicon. *Appl. Phys.* 52: 3622-3625.

Jasinski, J. M. and Chu, J. O. (1988). Absolute Rate Constants for the Reaction of Silylene with Hydrogen, Silane and Disilane. *J. Chem. Phys.* 88: 1678-1687.

Knights, J. C., Lucovsky, G. and Nemanich, R. J. (1979). Defects in Plasma-Deposited a-Si:H. *J. Non-Crystal. Solids*, 32: 393-403.

Knights, J. C. (1988). Plasma Deposition of a-Si:H. *Mat. Res. Soc. Symp. Proc.* 38: 371-381.

Krause, M., Topic, M., Stiebig, H. and Wagner, H. (2001). Thin Film UV Detectors Based on Hydrogenated Amorphous Silicon and Its Alloys. *Phys. Stat. Sol. A*, 185: 121-127.

Lifshitz, Y., Lempart, G. D., Grossman, E. (1994). Substation of Subplantation Model for Diamond-like Film Growth by Atomic Force Microscopy. *Phys. Rev. Lett.* 72: 2753-2756.

Longeway, P. A. (1984). Plasma Kinetics. *Semiconductors and Semimetals.* 21: 179-193.

Lucovsky, G., Nemarich, R. J. and Knights, J. C. (1979). Structural Interpretation of The Vibrational Spectra of a-Si:H Alloys. *Phys. Rev. B.* 19(4): 2064-2073.

Luft, W. and Tsuo, S. (1988). Plasma Deposition of Hydrogenated Amorphous Silicon Films. *Appl. Phys. Comm.* 8(1): 1-74.

Matsuda, A. and Tanaka, K. (1982). Plasma Spectroscopy-Glow Discharge Deposition of Hydrogenated Amorphous Silicon. *Thin Solid Films.* 92(1): 171-187.

Nishikawa, S., Kakinuma, H., Watanabe, T. and Nihei, K. (1985). Influence of Deposition Conditions on Properties of Hydrogenated Amorphous Silicon Prepared by RF Glow Discharge. *Jpn. J. Appl. Phys.* 24(6): 639-645.

Pankove, J. I. and Carlson, D. E. (1976). Electroluminescence in Amorphous Silicon. *Appl. Phys. Lett.*, 29(9): 620-628.

Patel, R. I., Olsen, D. J., Shrick, J. R. and Tran, N. T. (1986). Comparison Studies of Hydrogenated Amorphous Silicon Films Prepared from Silane-Hydrogen and Silane-Helium Mixtures. *Mat. Res. Soc. Symp. Proc.,* 70: 55-58.

Pincik, E., Kobayashi, H., Gleskova, H., Kucera, M., Ortega, L., Jergel, M., Falcony, C., Brunner, R., Shimizu, T., Nadazdy, V., Zeman, M., Mikula, M., Kumeda, M. and R.A.C.M.M. van Swaaij (2003). Photoluminescence Properties of a-Si:H Based Thin Films and Corresponding Solar Cells. *Thin Solid Films*, 433: 344-351.

Raizer, Y. R. (1991). *Gas Discharge Physics.* Berlin: Springer-Verlag.

Rand, M. (1979). Plasma-promoted Deposition of Thin Organic Films. *J. Vac. Sci. Tech..* 16(2): 420-427.

Reif, R., Kamins, T. I. and Saraswat, K. C. (1979). Surface Reactions in Discharge and CVD Deposition of Silane. *J. Electrochem. Soc.* 126: 644-652.

Reif, R. (1990). In: Rossnagel, S., Cuomo, J. and Westwood, W. ed. *Handbook of Plasma Processing Technology.* Park Ridge, N. J.: Noyes Publications. Ch. 10.

Robertson, R. and Gallagher, A. (1986). Reaction Mechanism and Kinetics of Silane Pyrolysis on a Hydrogenated Amorphous Silicon Surface. *J. Chem. Phys.* 85: 3623.

Ross, R. C., Jaklik, J. (1984). Plasma Polymerization and Deposition of Amorphous Hydrogenated Silicon from rf and dc Silane Plasmas. *J. Appl. Phys.,* 55(10): 3785-3794.

Sah, W. J., Lee, S. C., Tsai, H. K. and Chen J. H. (1990). Amorphous Silicon Edge Detectors for Application to Neural Network Image Sensors. *Appl. Phys. Lett.*, 56: 2539-2541.

Scott, B. A., Reimer, J. A. and Longeway, P. A. (1983). Growth and Defect Chemistry of Amorphous Hydrogenated Silicon. *J. Appl. Phys.* 54: 6853-6863.

Shen, D. S., Chatham, H. and Bhat, P. K. (1991). High-deposition Rate Amorphous Silicon Solar Cells: Silane or Disilane?. *Solar Cells*, 30: 271-275.

Sherman, A. (1984). Plasma-assisted Chemical Vapor Deposition Processes and Their Semiconductor Applications. *Thin Solid Films.* 113(2): 135-149.

Shimizu, T., Nakazawa, K., Kumeda, M., Ueda, S. (1983). *Physica (Utrecht)* 117B-118B: 926.

Sichanugrist, P., Suzuki, H., Konagai, M. and Takahashi, K. (1986). High-Rate Preparation of Amorphous-Silicon Solar Cells with Monosilane. *Jap. J. Appl. Phys.*, 25(3): 440-443.

Smith, D. L. (1994). *Thin Film Deposition.* New York: McGraw-Hill Inc..

Spear, W. E. and LeComber, P. G. (1975). Substitutional Doping of Amorphous Silicon. *Solid State Comm.* 17(9): 1193-1196.

Stein, H. J. (1975). Bonding and Thermal Stability of Implanted Hydrogen in Silicon. *J. Elec. Mater.* 4(1): 159-174.

Street, R. A. (1978). Recombination in Amorphous Semiconductors. *Phys. Rev. B*, 17: 3984-3995.

Street, R. A. (1991). *Hydrogenated Amorphous Silicon.* Cambridge: Cambridge University Press.

Tauc, J., Grigorovici, R. and Vancu, A. (1966). Optical Properties of Solids. *Phys. Stat. Sol.* 15: 627-638.

Thompson, L. F., Mayhan, K. G. (1972). The Plasma Polymerization of Vinyl Monomers. I. The Design, Construction and Operation of an Inductively Coupled Plasma Generator and Preliminary Studies With Nine Monomers. *J. Appl. Polym. Sci.* 16(9): 2291-2315.

Tong Li (2000). *Advanced Processes and Characterization of Amorphous Silicon Thin Film Transistors.* University of Michigan: Ph.D. Thesis.

Tsuo, T. S., Smith, E. B., Deb, S. K. (1987). Ion Beam Hydrogenation of Amorphous Silicon. *Appl. Phys. Lett.*, 51(18): 1436-1438.

Urbach, F. (1958). The Long-wavelength Edge of Photographic Sensitivity and the Electronic Absorption of Solids. *Phys. Rev.* 92(5): 1324.

Xi, J., Hollingsworth, R. E., Buitrago, R., Oakley, D., Cumalot, J. P., Naunberg, U., McNeil, J., Anderson, D. F. and Perez-Mendez, V. (1991). Minimum Ionizing Particle Detection Using Amorphous Silicon Diodes. *Nuclear Instruments & Methods in Physics Research*, A301: 219-222.

Yang, J., Banerjee, A. and Guha, S. (1997). Triple-junction Amorphous Silicon Alloy Solar Cell With 14.6% Initial and 13.0% Stable Conversion Efficiencies. *Appl. Phys. Lett.*, 70: 2975-2977.

Zhao, W. and Rowlands, J. A. (1995). X-ray Imaging Using Amorphous Selenium: Feasibility of a Flat Panel Self-scanned Detector for Digital Radiology. *Med. Phys.*, 22(10): 1595.

PRESENTATIONS

1. Conference On Advanced Material, Advanced Technology Congress 2003 (ATC2003), 20-21 May 2003, Putrajaya Marriot Hotel, IOI Resort, Putrajaya.

2. Conference on Public Institutions Of Higher Learning (IPTA), UPM, 9-10 October 2003, PWTC, Kuala Lumpur.

3. XX Regional Conference On Solid State & Technology (MASS), 12-14 December 2003, Lumut, Perak.

4. Annual Fundamental Science Seminar 2004 (AFSS 2004), 14-15 June 2004, Ibnu Sina Institute For Fundamental Science Studies, UTM Skudai, Johore.